Preferred Alignment of Mesochannels in a Mesoporous Silica Film Grown on a Silicon (110) Surface

Hirokatsu Miyata*,† and Kazuyuki Kuroda‡

Contribution from Canon Inc. R&D Headquarters Canon Research Center, 5-1, Morinosato-Wakamiya, Atsugi-shi, Kanagawa 243-0193, Japan, Department of Applied Chemistry, Waseda University, Ohkubo-3, Shinjuku-ku, Tokyo 169-8555, Japan, and Kagami Memorial Laboratory for Materials Science and Technology, Waseda University, Nishiwaseda-2, Shinjuku-ku, Tokyo 169-0051, Japan

Received March 8, 1999

Abstract: It has been proved that surfactant−silicate supramolecular architecture formed on a silicon substrate is strongly affected by the crystal orientation of a silicon wafer, indicating the variation of the interactions between the surfactants and the silicon surfaces. The hexagonal mesoporous silica film with aligned mesochannels was grown on a (110) wafer, whereas the mesochannels were not aligned in the films grown on (100) and (111) wafers. The alignment direction of the mesochannels on the (110) wafer is parallel to the [001] direction. The Gaussian distribution of the alignment direction with a full width at half-maximum (fwhm) of 29° was shown by in-plane X-ray diffraction. The hexagonal packing of the mesochannels in the film is distorted. The strong anisotropy of the atomic arrangement of silicon on the (110) surface causes the preferential alignment of mesochannels.

Introduction

Nanoscaled structural control of materials is one of the essential issues in diverse fields of chemistry and, in particular, it is a key technology for developing novel molecular devices. One of the rational methods to develop such nanostructured materials is to incorporate guest species into a host material with well-ordered nanospaces.[1−3] As a promising candidate for such ordered host materials, highly ordered mesoporous materials synthesized through the self-organization of surfactants and inorganic species have attracted considerable attention since the discovery of FSM-16 and MCM-41.[4−7]Several groups have reported the incorporation of guest species into mesoporous silica.[2,3,8−20]For the application to molecular devices, the film-forming ability of mesoporous silica[21−38] is a distinctive advantage. The potential of these films applicable to electronic

* Address correspondence to this author. E-mail: hiro@crc.canon.co.jp.
† Canon Inc. R&D Headquarters Canon Research Center.
‡ Waseda University.

(1) Alberti, G.; Bein, T. *Comprehensive Supramolecular Chemistry, Vol. 7; Solid-State Supramolecular Chemistry: Two- and Three-Dimensional Inorganic Networks*; Elsevier Science: UK, 1996; pp 1−772.
(2) Schöllhorn, R. *Chem. Mater.* **1996**, *8*, 1747−1757.
(3) Moller, K.; Bein, T. *Chem. Mater.* **1998**, *10*, 2950−2963.
(4) Yanagisawa, T.; Shimizu, T.; Kuroda, K.; Kato, C. *Bull. Chem. Soc. Jpn.* **1990**, *63*, 988−992.
(5) Inagaki, S.; Fukushima, Y.; Kuroda, K. *J. Chem. Soc., Chem. Commun.* **1993**, 680−682.
(6) Kresge, C. T.; Leonowicz, M. E.; Roth, W. J.; Vartuli, J. C.; Beck, J. S. *Nature* **1992**, *359*, 710−712.
(7) Beck, J. S.; Vartuli, J. C.; Roth, W. J.; Leonowicz, M. E.; Kresge, C. T.; Schmitt,K. D.; Chu, C. T.-W.; Olson, D. H.; Sheppard, E. W.; McCullen, S. B.; Higgins, J. B.; Schlenker, J. L. *J. Am. Chem. Soc.* **1992**, *114*, 10834−10843.
(8) Leon, R.; Margolese, D.; Stucky, G.; Petroff, P. M. *Phys. Rev. B: Condens. Matter* **1995**, *52*, r2285−r2288.
(9) Ko, C. H.; Ryoo, R. *Chem. Commun.* **1996**, 2467−2468.
(10) Ryoo, R.; Kim, J. M.; Ko, C. H.; Shin, C. H. *J. Phys. Chem.* **1996**, *100*, 17718−17721.
(11) Tang, Y. S.; Cai, S.; Jin, G.; Duan, J.; Wang, K. L.; Soyez, H. M.; Dunn, B. S. *Appl. Phys. Lett.* **1997**, *71*, 2448−2450.
(12) Srdanov, V. I.; Alxneit, I.; Stucky, G. D.; Reaves, C. M.; DenBaars, S. P. *J. Phys. Chem. B* **1998**, *102*, 3341−3344.
(13) Agger, J. R.; Anderson, M. W.; Pemble, M. E.; Terasaki, O.; Nozue, Y. *J. Phys. Chem. B* **1998**, *102*, 3345−3353.
(14) (a) Dag, Ö.; Kuperman, A.; Ozin, G. A. *Adv. Mater.* **1995**, *7*, 72−78. (b) Chomski, E.; Dag, Ö.; Kuperman, A.; Coombs, N.; Ozin, G. A. *Chem. Vap. Deposition* **1996**, *2*, 8−13.
(15) (a) Wu, C.-G.; Bein, T. *Chem. Mater.* **1994**, *6*, 1109−1112. (b) Wu, C.-G.; Bein, T. *Science* **1994**, *264*, 1757−1759.
(16) Ogawa, M. *Langmuir* **1995**, *11*, 4639−4641.
(17) Zhou, H. S.; Honma, I. *Chem. Lett.* **1998**, 973−974.
(18) Zhou, H. S.; Sasabe, H.; Honma, I. *J. Mater. Chem.* **1998**, *8*, 515−516.
(19) Corma, A.; Fornés, V.; García, H.; Miranda, M. A.; Sabater, M. J. *J. Am. Chem. Soc.* **1994**, *116*, 9767−9768.
(20) Lim, M. H.; Blanford, C. F.; Stein, A. *J. Am. Chem. Soc.* **1997**, *119*, 4090−4091.
(21) Ogawa, M. *J. Am. Chem. Soc.* **1994**, *116*, 7941−7942.
(22) Ogawa, M. *Chem. Commun.* **1996**, 1149−1150.
(23) Ogawa, M.; Igarashi, T.; Kuroda, K. *Bull. Chem. Soc. Jpn.* **1997**, *70*, 2833−2837.
(24) Ogawa, M. *Langmuir* **1997**, *13*, 1853−1855.
(25) Ogawa, M.; Ishikawa, H.; Kikuchi, T. *J. Mater. Chem.* **1998**, *8*, 1783−1786.
(26) Ogawa, M.; Kikuchi, T. *Adv. Mater.* **1998**, *10*, 1077−1080.
(27) Yang, H.; Kuperman, A.; Coombs, N.; Mamiche-Afara, S.; Ozin, G. A. *Nature* **1996**, *379*, 703−705.
(28) Aksay, I. A.; Trau, M.; Manne, S.; Honma, I.; Yao, N.; Zhou, L.; Fenter, P.; Eisenberger, P. M.; Gruner, S. M. *Science* **1996**, *273*, 892−898.
(29) Yang, H.; Coombs, N.; Sokolov, I.; Ozin, G. A. *J. Mater. Chem.* **1997**, *7*, 1285−1290.
(30) Martin, J. E.; Anderson, M. T.; Odinek, J.; Newcomer, P. *Langmuir* **1997**, *13*, 4133−4141.
(31) Lu, Y.; Ganguli, R.; Drewien, C. A.; Anderson, M. T.; Brinker, C. J.; Gong, W.; Guo, Y.; Soyez, H.; Dunn, B.; Huang, M. H.; Zink, J. I. *Nature* **1997**, *389*, 364−368.
(32) Zhao, D.; Yang, P.; Margolese, D. I.; Chmelka, B. F.; Stucky, G. D. *Chem. Commun.* **1998**, 2499−2500.
(33) Tolbert, S. H.; Schaffer, T. E.; Feng, J.; Hansma, P. K.; Stucky, G. D. *Chem. Mater.* **1997**, *9*, 1962−1967.
(34) Yang, H.; Coombs, N.; Sokolov, I.; Ozin, G. A. *Nature* **1996**, *381*, 589−592.
(35) Yang, H.; Coombs, N.; Dag, Ö.; Sokolov, I.; Ozin, G. A. *J. Mater. Chem.* **1997**, *7*, 1755−1761.
(36) Yang, H.; Coombs, N.; Ozin, G. A. *J. Mater. Chem.* **1998**, *8*, 1205−1211.
(37) Yang, H.; Ozin, G. A.; Kresge, C. T. *Adv. Mater.* **1998**, *10*, 883−887.

10.1021/ja990758m CCC: $18.00 © 1999 American Chemical Society
Published on Web 08/06/1999

devices will be greatly improved if the formation of the films with perfectly aligned mesochannels was achieved on an electrically conductive stable substrate. For example, mesoporous silica films without an azimuthal alignment of mesochannels are less useful for the fabrication of 1-dimensional conductor through incorporation of metals, since the total conductivity of the film becomes isotropic even though the local anisotropy of the conductivity was achieved.

Several attempts have been performed to obtain mesoporous silica films with aligned mesochannels on substrates.[39−42] The alignment of mesochannels was achieved by the methods using a flow of the reactants.[39,40] However, these methods require special apparatus and restrict the shapes and properties of the substrates. Although the local alignment of mesochannels was reported on mica and graphite substrates,[27−29] the alignment over the whole area has not been achieved, and on top of that, these substrates are not appropriate for practical use. Recently, Zhao et al. reported the formation of mesoporous silica films with aligned mesochannels onto silicon wafers by dip-coating.[42] However, the templating materials used in their experiments were limited to specialized nonionic surfactants such as block copolymers. Moreover, the possibility that the interior region of the film has a disordered structure cannot be excluded as has been demonstrated by Lu et al.[31]

Here, we report the formation of a mesoporous silica film with highly aligned mesochannels on a silicon (110) substrate. The film was prepared by the epitaxial-like growth from a reactant solution. The alignment of the mesochannels in the film was confirmed by in-plane X-ray diffraction[43] and high-resolution scanning electron microscopy (HRSEM). Moreover, the alignment over the whole film thickness was proved by cross-sectional transmission electron microscopy (TEM). The 2-fold symmetric arrangement of the silicon atoms on the (110) surface caused the preferred alignment. This was supported by the fact that the mesochannels in the silica films grown on silicon (111) and (100) substrates under the same conditions were not aligned.

Experimental Section

Materials. Phosphorus-doped n-type (100) wafers with the resistivity of 0.001−0.02 Ωcm and nondoped (111) wafers were obtained from Mitsubishi Material Silicon Co., and phosphorus-doped n-type (110) wafers with the resistivity of 1−2 Ωcm were obtained from Japan Silicon Co. Cationic surfactant hexadecyltrimethylammonium chloride ($CH_3(CH_2)_{15}N(CH_3)_3Cl$) abbreviated as CTACl was obtained from Tokyo Chemical Industry Co. Tetraethoxysilane, ($(C_2H_5O)_4Si$) abbreviated as TEOS, with >96% purity was obtained from Tokyo Chemical Industry Co. Hydrochloric acid with 35−37% concentration was obtained from Kokusan Chemical Co. All the chemicals were used as received.

Synthesis. The mesoscopic silica film formation was performed through the hydrolysis of silicon alkoxide in the presence of surfactants under the acidic conditions as reported by Yang et al.[27] TEOS was mixed with an acidic cationic surfactant CTACl solution and the mixture was stirred for 2−3 min at room temperature and transferred into a Teflon vessel that contains substrates. The molar ratio was 0.10 TEOS: 0.11 CTACl:100 H_2O:10.5 HCl. Silicon wafers with (100), (111), and (110) orientations were used as substrates. Each silicon substrate (typical size of 12 mm × 12 mm) was held horizontally in the vessel between two Teflon disks with the polished surface downward. The lower disk has a 10 mm × 10 mm window and the wafer surface is exposed to the reactants through the window. The silicon surfaces were treated with a 1% hydrofluoric acid solution to remove the native oxide layers prior to the reaction. The vessel was sealed at 80 °C for 1 day to 1 week for the formation of mesoporous silica films. The thickness of the films was not controlled because of a nonlinearity of the thickness with the reaction time. The samples were washed with distilled water and air-dried. The calcination of the samples was conducted in a muffle furnace at 540 °C for 10 h at a temperature rate of 2 °C/min.

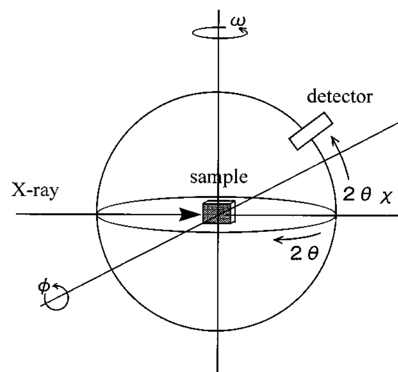

Figure 1. Illustration of the four axes of the goniometer used in the in-plane XRD measurement.

Instrumentation. Standard $\theta-2\theta$ X-ray diffraction (XRD) data were recorded on a Rigaku RAD-2R diffractometer using Cu Kα radiation with a graphite monochromator. A grazing angle in-plane XRD study[43] was performed on a X-ray diffractometer equipped with a 4-axes goniometer (Rigaku ATX-G) with a parabolic multilayer mirror as a primary beam condenser. Cu Kα radiation from a copper rotating anode was used for the experiment. The four axes of the goniometer are illustrated in Figure 1. Scanning electron microscopic images were recorded on a Hitachi S-900 microscope at an accelerating voltage of 25 kV without a metal coating on the specimen. Transmission electron microscopic images were recorded on an Akashi 002B microscope at an accelerating voltage of 100 kV. The specimen for the cross-sectional TEM observation was prepared as follows; first, the sample was embedded in an epoxy resin and was sawed into a piece with a thickness of ~500 μm; second, the piece was mechanically prethinned and polished by a disk grinder and a dimple grinder to produce a central region ~10 μm thick; and finally, the central region was milled with an Ar^+ ion beam of 5 keV energy with incident angles between −1 and 4°. The images by atomic force microscopy (AFM) were recorded on a Digital-Instruments D3000 tapping AFM system using a super sharp tip (nominal tip end radius of curvature: 2−5 nm) with a scanning area of 200 nm square.

Results and Discussion

Glossy continuous mesoporous silica films with 0.1−0.2 μm thickness were grown onto the substrates. The as-grown films were crack-free over the whole area and hard to peel off from the substrates.

Mesochannel Structure. The mesoscopic structure of the films was confirmed by XRD. The film sample on each substrate showed (100) and (200) diffraction peaks of the hexagonal mesoporous structure at $2\theta = 2.3$ and 4.6, though no (110) peak was observed, indicating the hexagonal channels run parallel to the silicon surface as has already been demonstrated on mica and graphite substrates (Figure 2, trace A).[27,29] The center-to-center distance of the channels was calculated to be ~4.4 nm from the d_{100} spacing. The retention of the channel structure over the calcination was confirmed by the existence of the (100) XRD peak obtained for the calcined film, but a contraction of

(38) Schacht, S.; Huo, Q.; Voigt-Martin, I. G.; Stucky, G. D.; Schüth, F. *Science* **1996**, *273*, 768−771.
(39) Hillhouse, H. W.; Okubo, T.; van Egmond, J. W.; Tsapatsis, M. *Chem. Mater.* **1997**, *9*, 1505−1507.
(40) Trau, M.; Yao, N.; Kim, E.; Xia, Y.; Whitesides, G. M.; Aksay, I. A. *Nature* **1997**, *390*, 674−676.
(41) Tolbert, S. H.; Firouzi, A.; Stucky, G. D.; Chmelka, B. F. *Science* **1997**, *278*, 264−268.
(42) Zhao, D.; Yang, P.; Melosh, N.; Feng, J.; Chmelka, B. F.; Stucky, G. D. *Adv. Mater.* **1998**, *10*, 1380−1385.
(43) Marra, W. C.; Eisenberger, P.; Cho, A. Y. *J. Appl. Phys.* **1979**, *50*, 6927−6933.

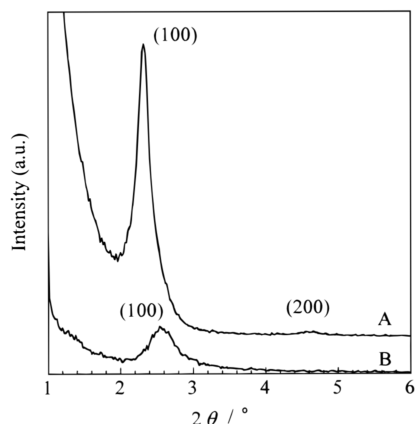

Figure 2. XRD patterns of the mesoporous silica film grown on the silicon (110) wafer. Conventional $\theta-2\theta$ scan. (A) As-synthesized film and (B) calcined film.

the *d* spacing by ∼0.3 nm and the decrease in the diffraction intensity were observed (Figure 2, trace B). This observation implies the condensation of residual hydroxyls in the wall and the disordering of the mesoporous structure. The calcination did not cause a crack on the film, thus a continuous hollow mesoporous silica film was obtained.

Preferred Alignment of Mesoporous Silica. The observations by optical microscopy and SEM reveal the morphological difference of the films formed on the silicon substrates with different crystal orientations. For the films grown on the (100) and (111) wafers, the winding striped contrast corresponding to the grain boundary was observed over the whole film by an optical microscope, whereas the aligned ellipsoid-shaped texture was observed on the overall film grown on the (110) wafer instead. SEM observations revealed that the aligned texture on the (110) wafer corresponds to the alignment of the micrometer-sized mesoporous silica domain. Similar aligned texture has been observed on the mesoporous silica film grown on a mica substrate.[27] The morphological difference of the films is distinctive at the edges of the films; preferred alignment of the domains was observed on the (110) surface (Figure 3a), whereas the random connection of the curled mesoporous silica domains was observed on the (100) and (111) surfaces (Figure 3b). These results indicate the preferential alignment of mesoporous silica

Figure 3. SEM images of the as-synthesized mesoporous silica films on the silicon substrates: (a) low magnification image of the film on the (110) wafer, (b) low magnification image of the film on the (111) wafer, (c) high magnification image of the film on the (110) wafer, and (d) high magnification image of the film on the (111) wafer.

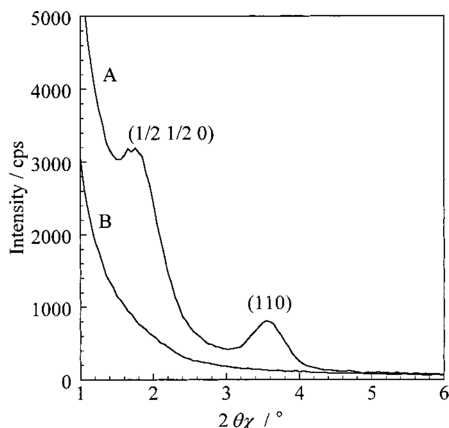

Figure 4. $\phi - 2\theta\chi$ scan profile (in-plane XRD) of the as-synthesized mesoporous silica film on the silicon (110) wafer. The alignment direction of the mesoporous silica domains was set (A) parallel and (B) normal to the direction of incident X-rays at $\phi = 0°$.

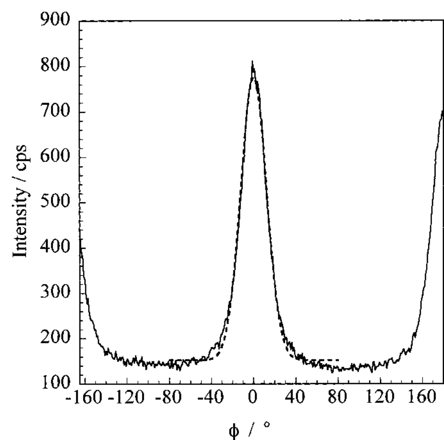

Figure 5. ϕ scan profile (in-plane XRD) of the as-synthesized mesoporous silica film on the silicon (110) wafer. The detector is set at the (110) peak maximum of the $\phi - 2\theta\chi$ profile in Figure 4. Dotted line: Gaussian fitted curve. The fwhm of the distribution of the alignment direction was estimated to be 29°.

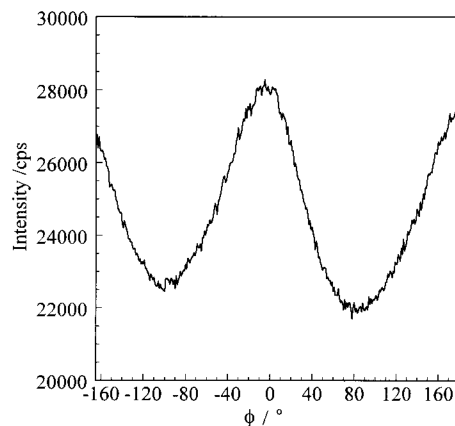

Figure 6. ϕ angle dependence of the (100) peak intensity of the as-synthesized mesoporous silica film on the silicon (110) wafer.

on the silicon (110) surface. No substantial morphological difference was observed between the as-synthesized film and the calcined film.

The alignment of the mesochannels in the film was directly observed by HRSEM. As silicon substrates are conductors, the observation with a high accelerating voltage is possible without a metal coating on the specimen. Figure 3c is the high magnification image of the as-synthesized mesoporous silica film grown on the (110) wafer. Stripes with a ~5 nm interval were observed at the edge of each mesoporous silica domain. This result shows that the hexagonal mesochannels run parallel to the long axis of the mesoporous silica domain. The observed hierarchical alignments of mesoporous silica clearly show the total alignment of the mesochannels over the whole film grown on the (110) surface. For the round mesoporous silica domain formed on the (111) wafer, observed curved channels indicate the random orientation of the mesochannels in the film (Figure 3d).

In-plane X-ray diffraction study was conducted to obtain direct evidence of the total alignment of the mesochannels over the whole surface. The direct evidence for the alignment of the mesochannels in the film is not available using conventional $\theta - 2\theta$ measurements because only the structural information parallel to the film surface is obtainable. In-plane X-ray diffraction is caused by the lattice planes normal to the film surface when the X-rays are impinged to the sample surface at a grazing angle around the total reflection angle.[43] Figure 4 is the $\phi - 2\theta\chi$ scan profile of the as-synthesized mesoporous silica film grown on the silicon (110) wafer. Traces A and B were recorded with the sample orientations that the alignment direction of the mesoporous silica domains was set parallel and normal to the direction of the incident X-rays at $\phi = 0°$, respectively. In trace A, two diffraction peaks are observed at $2\theta\chi = 1.75°$ and 3.55°, corresponding to the lattice spacings of 5.05 and 2.49 nm, respectively. These diffraction peaks were assigned to be (1/2, 1/2, 0) and (110), respectively, based on the mesochannel arrangement deduced from the fact that the (110) peak is not observed in the conventional $\theta - 2\theta$ XRD pattern (Figure 2). Because the penetration depth of the grazing incident X-rays is very shallow in this measurement, this in-plane diffraction is caused by the surface thin layer. This is the reason that the diffraction corresponding to the center-to-center distance of the hexagonal mesoporous structure was directly observed. On the other hand, no diffraction peaks were observed in trace B. These results obviously indicate the preferential alignment of the (110) plane over the whole mesoporous silica film.

For the quantitative estimation of the degree of the preferential alignment of the mesochannels, a ϕ scan was conducted fixing the detector position ($2\theta\chi$) at the (110) diffraction peak maximum. The ϕ scan profile for the as-synthesized film is shown in Figure 5. Two diffraction peaks were observed with an interval of 180°. This profile can fit the Gaussian curve, indicating the direction of the in-plane alignment of the mesochannels shows Gaussian-type distribution. The fwhm of the distribution of the alignment direction was estimated to be 29°, showing highly preferential alignment of the mesochannels. The ϕ scan profile recorded at $2\theta\chi = 1.8°$ showed a tendency similar to that shown in Figure 5. It is worth noting that the ϕ scan profile of the (100) peak intensity measured with a conventional $\theta - 2\theta$ scanning arrangement also showed a similar variation of the diffraction intensity (Figure 6). The observed rotation angle dependence of the (100) peak intensity would reflect the anisotropy of the "crystallite", i.e., anisotropy of the individual silicate rod that builds up the mesoporous silica film. Although the profiles of Figures 5 and 6 are similar, the ϕ scan profile in Figure 6 includes no direct information on the alignment of the mesochannels.

The center-to-center distance of the mesochannels estimated by in-plane XRD (5.0 nm) was larger than that calculated from the d_{100} spacing measured by conventional XRD (4.4 nm). This

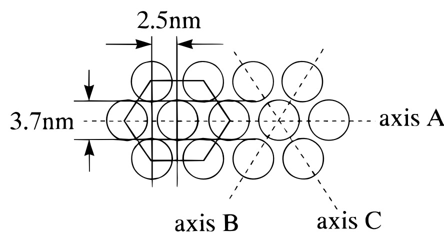

Figure 7. Schematic illustration of the mesochannel arrangement in the mesoporous silica film grown on the silicon (110) wafer. The distance along the axis A is longer than the distances along axes B and C.

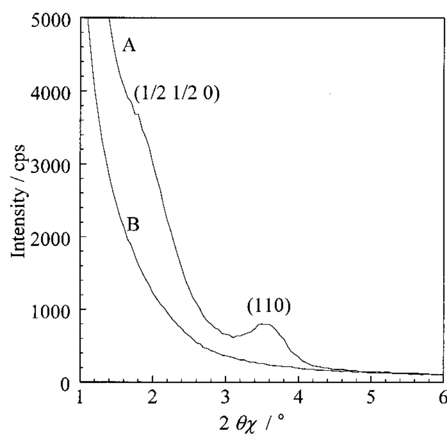

Figure 8. $\phi-2\theta\chi$ scan profile (in-plane XRD) of the calcined mesoporous silica film on the silicon (110) wafer. The alignment direction of the mesoporous silica domains was set (A) parallel and (B) normal to the direction of incident X-rays at $\phi = 0°$.

inconsistency indicates that the hexagonal mesoporous structure in the film grown on the (110) wafer is distorted. The arrangement of the mesochannels is schematically illustrated in Figure 7. The lateral distance (along the A axis) is longer than the distances along the other two axes (axes B and C). The deviation from the ideal hexagonal channel structure was estimated to be 11%, indicating a larger distortion of the mesoporous silica film than that on mica.[28]

The retention of the alignment of the mesochannels in the film over the calcination was confirmed by in-plane XRD. Figures 8 and 9 are the $\phi-2\theta\chi$ scan profile and the ϕ scan profile of the calcined mesoporous silica film, respectively. In Figure 8, traces A and B were recorded with the sample orientations that the alignment direction of the mesoporous silica domains was set parallel and normal to the direction of the incident X-rays at $\phi = 0°$, respectively. Two diffraction peaks were observed in trace A and no diffraction peaks were observed in trace B, showing the retention of the mesochannel alignment. It is worth noting that the positions of the two diffraction peaks in the $\phi-2\theta\chi$ profiles (Figures 4 and 8) are identical. This indicates that the horizontal distance of the mesochannels is unchanged by the calcination. The strong adhesion of the mesoporous silica onto the substrate prevents the film from undergoing horizontal shrinking. This is not inconsistent with the shrinkage observed in Figure 2, because the structural information obtained by a $\theta-2\theta$ scan is vertical to the substrate. The fwhm of the ϕ scan profile of the calcined film (Figure 9) was estimated to be 26°, which confirms the complete retention of alignment of the mesochannels in the film.

The alignment of the mesochannels in the film grown on the (110) wafer is also evidenced by the cross-sectional TEM image. Figure 10 is the cross-sectional TEM image of the as-synthesized mesoporous silica film on the (110) wafer sliced perpendicular

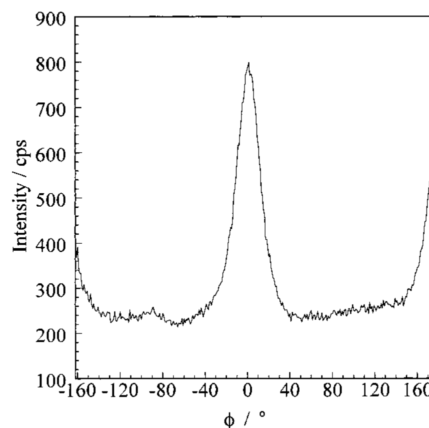

Figure 9. ϕ scan profile (in-plane XRD) of the calcined mesoporous silica film on the silicon (110) wafer. The detector is set at the (110) peak maximum of the $\theta-2\theta\chi$ profile in Figure 8. The fwhm of the distribution of the alignment direction was estimated to be 26°.

to the long axes of the mesoporous silica domains. The hexagonal mesoporous structure was clearly observed over all thicknesses of the film, showing a complete alignment of the mesochannels. The distortion of the hexagonal packing is also evident from this TEM image itself and the 2-dimensional Fourier transformation pattern of the image (Figure 10, inset). The center-to-center distance of the mesochannels parallel to the substrate surface (along the A axis in Figure 7) was estimated to be ~5 nm. This is longer than the distances along the other two directions (axes B and C) and is consistent with the distance measured by in-plane XRD.

To investigate the alignment of mesochannels at the silicon–water interface, the region without a thick film growth was examined. Figure 11 is the HRSEM image of the aligned first layer of mesoporous silica on the silicon (110) surface. The sample used in this HRSEM observation is an edge part of the film, i.e., the region that was not exposed to the reactants directly by being covered by a Teflon disk. However, the surface of this region can contact with a small amount of the reactants by capillary action, so a very small amount of mesoporous silica was precipitated in this region. Stripes with a ~5 nm interval were observed. Although the stripes are meandering and partially disordered, the total orientation was the same in each part of the sample and almost parallel to the long axes of the mesoporous silica domains. Stripes with a ~5 nm interval were also observed by AFM (not shown), and the interval was estimated to be 5.0 nm from its 2-dimensional Fourier transformation image. The observed interval coincides with the center-to-center distance estimated by in-plane XRD and cross-sectional TEM. The measurement of the height of the striped structure was unsuccessful because of the insufficient resolution of the AFM tip.

The Alignment Effect of the Silicon (110) Surface. As shown in Figure 11, the stripes of the first layer of the mesoporous silica are meandering. On the other hand, the Gaussian-type distribution of the alignment direction with the fwhm of 29° is shown by in-plane XRD (Figure 5). As has been reported in the earlier work on mesoporous silica films grown on mica and graphite substrates,[28] the distribution of the alignment direction is strongly influenced by the interactions between the substrate surfaces and surfactant molecules. The mesochannels are meandering on a mica substrate where the small interaction area is expected, whereas the rigid parallel mesochannels without the meandering curvature are observed on a graphite substrate where the interaction area is expected

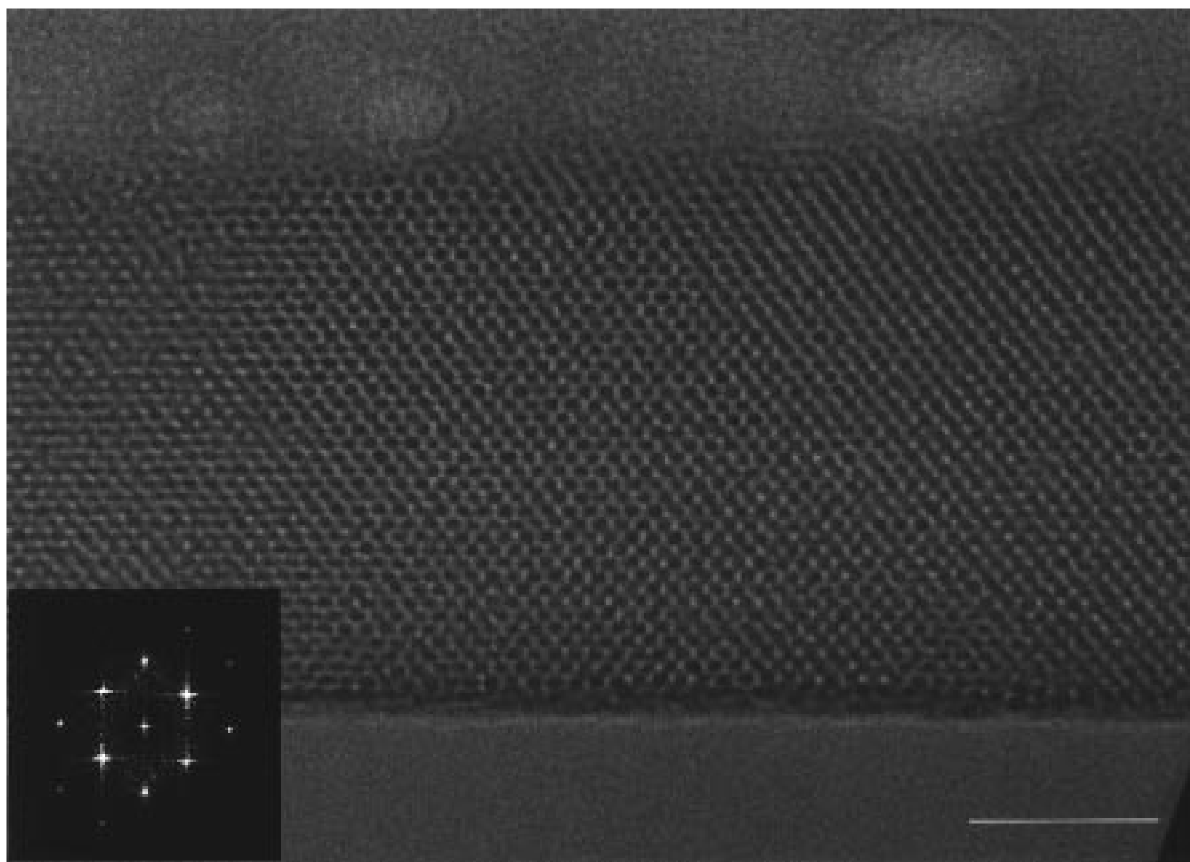

Figure 10. Cross-sectional TEM image of the as-synthesized mesoporous silica film grown on the silicon (110) wafer. The image was recorded at an accelerating voltage of 100 kV (scale bar; 50 nm). The sample was sliced perpendicular to the long axes of the mesoporous silica domains. Inset: The 2-dimensional Fourier transformation image of the mesoporous silica part.

to be large.[28] Therefore, the observed distribution of the direction of mesochannel alignment on the silicon (110) substrate shows a small alignment effect of the silicon surface. The surface of silicon provides SiOH anchoring sites which are expected to interact with the headgroups of the surfactants. This small interaction area gives rise to a small alignment effect and causes both the meandering stripes and the observed distribution of the alignment direction.

The alignment of mesoporous silica only on the (110) surface is indicative of the presence of an optimum atomic arrangement on the surface for the interactions with the surfactants. Crystallographic consideration for a diamond-type crystal shows that the atomic arrangement on the (110) surface has a strong anisotropy compared to the arrangements on the (100) and (111) surfaces; ⟨111⟩ is a 3-fold axis and ⟨100⟩ is a 4-fold axis of symmetry, whereas ⟨110⟩ is a 2-fold axis of symmetry, i.e., a specific azimuthal direction can be defined on (110). Probably this strong anisotropic atomic arrangement on the (110) surface causes the preferred alignment of the mesochannels. Since a silicon surface is readily oxidized in air, silicon atoms do not directly participate in the interactions with the surfactants. The regular arrangement of silanols on the surface should be responsible.

The Alignment Direction on the Silicon (110) Surface. The following three experiments were performed to describe the alignment direction in the crystallographic axes of silicon.

At first, the electron channeling pattern (ECP)[44] of the underlying silicon substrate was observed for the sample where

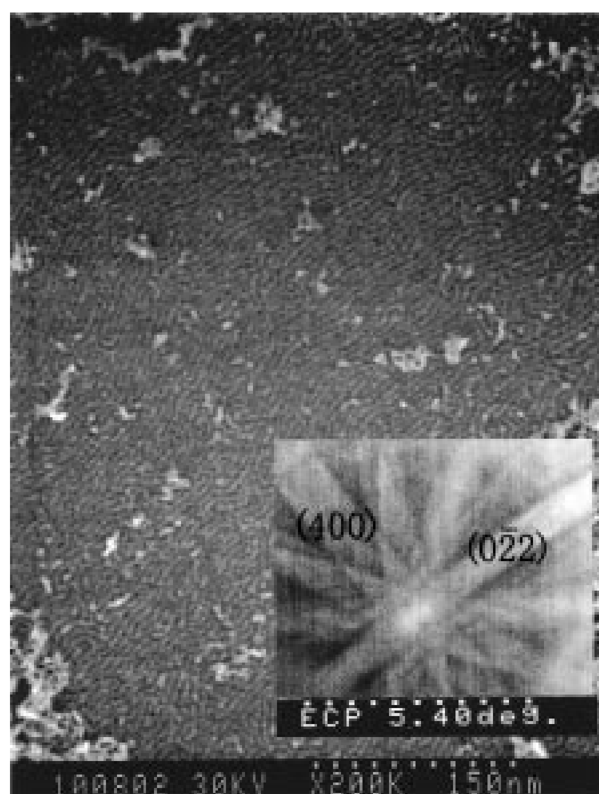

Figure 11. HRSEM image of the aligned first layer of the as-synthesized mesoporous silica on the silicon (110) surface. Inset: ECP pattern of the underlying silicon substrate at the same position.

(44) Newbury, D. E.; Joy, D. C.; Echlin, P.; Fiori, C. E.; Goldstein, J. I. *Advanced Scanning Electron Microscopy and X-ray Microanalysis*; Plenum Press: New York, 1986; pp 87−145.

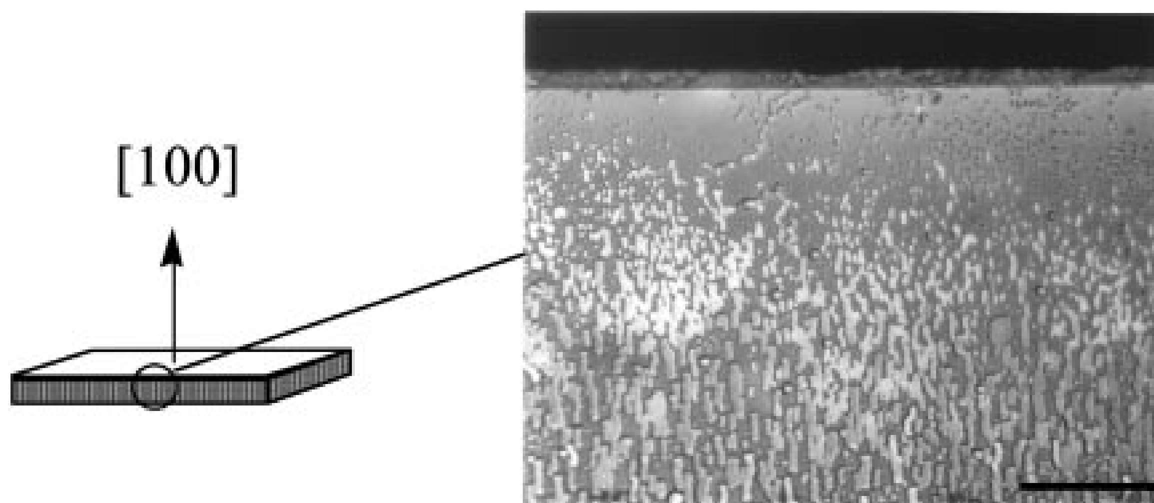

Figure 12. Optical microscopic image of the as-synthesized mesoporous silica on the cleaved (110) side surface of the (100) wafer. The long axes of the domains are parallel to the normal of the wafer surface, [100]. Scale bar, 20 μm.

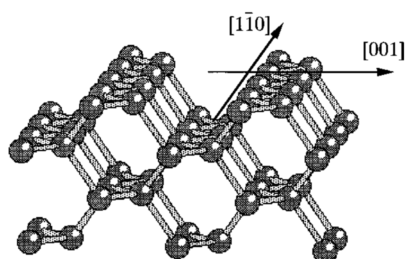

Figure 13. Schematic drawing of the atomic arrangement on a silicon (110) plane. The mesoporous silica align along the [001] axis. Zigzag arrays of the silicon atoms and channels are along the [1$\bar{1}$0] axis.

the alignment direction of the mesochannels is shown. The ECP image of the substrate was recorded for the region without a thick mesoporous silica film because it is impossible to observe the ECP image over the thick film. The ECP image of the silicon substrate at the same point as Figure 11 is shown in the inset of Figure 11. This ECP image is typical for the silicon {110} surface. The comparison of the ECP image with the SEM image shows that the total direction of the alignment of mesochannels is nearly normal to the (400) pattern, i.e., nearly parallel to the [001] direction.

Second, the mesoporous silica film forming on a cleaved (110) surface, which is a side surface of the (100) wafer, was investigated (Figure 12). The cleaved surfaces of the silicon (100) wafer are (011) and (0$\bar{1}$1) and these are equivalent to (110). The alignment of the mesoporous silica domain on the cleaved surface is shown in Figure 12. It is evident that the alignment direction is parallel to the substrate normal, indicating the domains are aligned along the [100].

Third, the electron diffraction pattern was observed for the silicon substrate of the sample used for the cross-sectional TEM observation shown in Figure 10. The diffraction pattern (not shown here) corresponding to the {100} orientation was clearly observed. This shows that the alignment axis of the mesochannels is parallel to the [001] axis and is consistent with the above two experimental results.

All of these results clearly show that the alignment direction on the (110) surface is fixed to the [001] axis of the silicon crystal. The arrangement of the silicon atoms on the (110) surface is schematically illustrated in Figure 13. As shown in Figure 13, zigzag arrays of silicon atoms are aligned along [1$\bar{1}$0] and channels run between the arrays. Accordingly, the distance between the surface silanol groups shows a strong anisotropy on the (110) surface. The alignment direction of the mesochannels, [001], corresponds to the direction that the distance between the silanol groups is longest. This anisotropic arrangement of the silanols on the (110) surface which interact with the headgroups of surfactants is responsible for the preferential alignment of mesoporous silica.

Conclusion

The variation of the surfactant−silicate supramolecular architecture formed on crystalline surfaces with different crystal orientations was proved for the first time. A continuous hexagonal mesoporous silica film with azimuthally aligned mesochannels was obtained through the epitaxial-like growth of mesoporous silica seeds on the (110) surface of single-crystal silicon, whereas no preferential mesochannel alignments were observed for the films grown on the (100) and (111) surfaces. The strong anisotropy of the arrangement of the silanol groups on the (110) surface causes the observed alignment of mesochannels. The observed strong influence of the surface atomic arrangements on the morphology of the mesoporous silica films indicates that the morphological control is realized through various artificial surface modifications. The mesoporous silica film on a substrate with preferentially aligned mesochannels is a promising candidate for the host material of novel molecular devices developed through incorporation of various guest species such as metals, semiconductors, organic dyes, and so on.

Acknowledgment. The authors acknowledge Dr. K. Inaba (Rigaku Co. X-ray Research Laboratory) for the in-plane XRD measurements. The authors also acknowledge Mr. S. Kobayashi, Mr. M. Watanabe, and Mr. S. Yoshida (Canon Inc. Canon Research Center) for the cross-sectional TEM observation and AFM measurement.

JA990758M